

## ARTICLE OPEN



# *Npbwr1* signaling mediates fast antidepressant action

Gregor Stein<sup>1</sup>, Janine S. Aly<sup>2</sup>, Lisa Lange<sup>1</sup>, Annamaria Manzolillo<sup>2</sup>, Konstantin Riege<sup>3</sup>, Anna Brancato<sup>4</sup>, Christian A. Hübner<sup>2</sup>, Gustavo Turecki<sup>5</sup>, Steve Hoffmann<sup>3</sup> and Olivia Engmann<sup>1,2</sup>✉

© The Author(s) 2024

Chronic stress is a major risk factor for depression, a leading cause of disability and suicide. Because current antidepressants work slowly, have common side effects, and are only effective in a minority of patients, there is an unmet need to identify the underlying molecular mechanisms. Here, we identify the receptor for neuropeptides B and W, *Npbwr1*, as a key regulator of depressive-like symptoms. *Npbwr1* is increased in the nucleus accumbens of chronically stressed mice and postmortem in patients diagnosed with depression. Using viral-mediated gene transfer, we demonstrate a causal link between *Npbwr1*, dendritic spine morphology, the biomarker *Bdnf*, and depressive-like behaviors. Importantly, microinjection of the synthetic antagonist of *Npbwr1*, CYM50769, rapidly ameliorates depressive-like behavioral symptoms and alters *Bdnf* levels. CYM50769 is selective, well tolerated, and shows effects up to 7 days after administration of a single dose. In summary, these findings advance our understanding of mood and chronic stress and warrant further investigation of CYM50769 as a potential fast-acting antidepressant.

*Molecular Psychiatry*; <https://doi.org/10.1038/s41380-024-02790-4>

## INTRODUCTION

Depression (major depressive disorder) affects up to 1 in 7 people in high-income countries within their lifetime [1–3]. Associated illnesses are among the largest categories of healthcare expenditure [4, 5]. While a growing battery of antidepressant drugs is available, only ketamine has a fast-acting mechanism. Because current antidepressants work slowly, are only partially effective, and have common side effects [6–8], there is an unmet need to identify other, fast-acting pathways, to rapidly ameliorate symptoms of stress and depression in ways independent of known signaling such as serotonergic and glutamatergic signaling.

Chronic stress and depression share molecular signatures that can be modeled reliably in mice [9, 10]. Rapid environmental interventions such as dietary factors are known to impact symptoms of stress and depression but the underlying mechanisms are not fully elucidated [11]. Here we used caffeine, a rapid mood-elevator in mice, [12] as a tool to identify pathways linked to mood and associated disorders. Caffeine alters diurnal gene expression and mood via the interaction of Thr75-DARPP-32 and the CLOCK/BMAL transcription factor complex [12]. However, the downstream gene products, which may mediate mood-elevating effects of caffeine, remain unknown.

Using RNA sequencing, we pinpoint the receptor for neuropeptides B and W (*Npbwr1*, also called GPR7) as a mediator of mood-elevating and antidepressant-like effects in mice. Both NPB and NPW are produced by brain areas projecting to the Nucleus accumbens (NAc), including the ventral tegmental area and the dorsal raphe nuclei [13, 14], which are implicated in chronic stress and depression.

*Npbwr1* is increased by chronic variable stress (CVS) and *NPBWR1* is elevated postmortem in the NAc of depressed patients. Using viral-mediated gene transfer, we identify a causal link between *Npbwr1* and depression-related phenotypes. RNA-sequencing after viral overexpression of *Npbwr1* provides a link to *Bdnf*, a key gene in the antidepressant response [15]. Microinjection of the synthetic *Npbwr1*-antagonist CYM50769 into the NAc reversed the behavioral effects of chronic stress and altered *Bdnf* levels for up to 7 days after one single dose. Accordingly, microinjection of the natural agonist NPB mimicked chronic stress effects and had an opposing effect on *Bdnf*.

In summary, these data characterize a previously unknown pathway, which has rapid effects on stress- and depression-related behaviors. We propose that CYM50769, a selective and well-tolerated molecule, may have fast-acting antidepressant-like effects in mice that warrant further investigation.

## METHODS

Further information can be found in the *extended methods*.

## Animals and licenses

Mice were housed following the ethical guidelines of the Thüringer Landesamt für Verbraucherschutz (TLV). Experiments were conducted under animal licenses UKJ-18-036 and UKJ-21-012 (Germany), which comply with the EU Directive 2010/63/EU guidelines for animal experiments. Experiments with genetically modified organisms were performed according to S1 regulations according to the GenTAufzV. PPP1R1B (DARPP-32) T75A knock-in mice were described in [12, 16]. C57Bl/6J mice were housed and bred in the

<sup>1</sup>Institute for Biochemistry and Biophysics, Friedrich-Schiller-University Jena, Jena, Germany. <sup>2</sup>Institute of Human Genetics, Jena University Hospital, Am Klinikum 1, F2E20, 07747 Jena, Germany. <sup>3</sup>Computational Biology Group, Leibniz Institute on Aging - Fritz Lipmann Institute (FLI), Beutenbergstraße 11, 07745 Jena, Germany. <sup>4</sup>Department of Health Promotion, Mother and Child Care, Internal Medicine and Medical Specialties, University of Palermo, Palermo, Italy. <sup>5</sup>Douglas Mental Health University Institute, Department of Psychiatry, McGill University, Montreal, QC, Canada. ✉email: [olivia.engmann@uni-jena.de](mailto:olivia.engmann@uni-jena.de)

Received: 22 March 2024 Revised: 3 October 2024 Accepted: 8 October 2024

Published online: 21 October 2024

animal facility (FZL) of the Universitätsklinikum Jena, Germany, and in the BIZ animal facility of Friedrich-Schiller-University Jena, Germany, or purchased from Janvier Labs (Saint Berthevin Cedex, France). Both sexes were used as stated. Mice were at least 8 weeks old and were housed in a 12L:12D light cycle.

### Drugs and chemicals

Mice were intraperitoneally (i.p.) injected with 7.5 mg/kg caffeine (#, C0750, Sigma) or saline at an injection volume of 10 ml/kg body weight and tested 2 or 24 h later [12, 17]. NPB ((#CSB-MP015971HU-100, Cusabio) was injected at doses of 1, 3, and 10 nM into the NAc. NPB was diluted in ddH<sub>2</sub>O up to 100 nM and then diluted with artificial cerebrospinal fluid, which also served as a control. CYM50769 (#4948, Tocris) was injected into the NAc at doses of 0.1 – 10 μM. CYM50769 was diluted in DMSO up to 100 μM and then diluted in artificial cerebrospinal fluid, which also served as a control solution containing the proper concentration of DMSO (#3525, Tocris).

### RNA purification and quantification

RNA was purified by resuspension in Trizol and chloroform-precipitation. RNA was washed in isopropanol and 75% Ethanol. After cDNA conversion with a GoScript™ Reverse Transcriptase kit (#A5001, Promega), quantitative real-time PCR was performed on a Bio-rad CFX96 Real-time system. Primer sequences are listed in the supplementary material. Quantitative PCR results were processed as described [18].

### Western blot and antibodies

Proteins were sonicated for 10 s in 1% SDS and denatured at 98 °C for 5 min. Laemmli buffer was added (100 mM Tris-HCl, pH 6.8, 12% glycerol, 40 g l<sup>-1</sup> SDS, 2% β mercaptoethanol, and bromphenol blue) and the samples were heated for another 5 min [16]. They were resolved by SDS-PAGE using a Bio-rad system and 4–15% Mini-PROTEAN TGX Precast Protein Gels (#4561086, Bio-rad) and transferred to nitrocellulose membranes (pore size 0.45 μm, #GE10600002, Amersham). Membranes were blocked for 1 h in 1% bovine serum albumin in TBS-T (Tris-buffered saline with Tween, 20 mM Tris, 150 mM NaCl, 0.1% Tween 20, pH 7.5) and incubated overnight at 4 °C with primary antibody (Anti-GPCR CPR7/NPBWR1 antibody, 0.5 μg/ml, #A08247-1, Boster Bio; Actin, 1/1,000, #A-5441, Sigma). Membranes were washed at RT 4x for 15 min in TBS-T, followed by 1 h incubation with the respective secondary antibody at RT (HRP-conjugated anti-rabbit, 1/4,000, #NA9340, GE Healthcare; HRP-conjugated anti-mouse, 1/3,000, #NA9310, GE Healthcare). An immune signal was detected using Clarity Western ECL substrate (#1705061, Bio-Rad) and a LAS 4000 automated detection system (GE Healthcare). Bands were quantified in ImageJ.

### AAVs, stereotaxic surgery, and microinjection

Bilateral stereotaxic surgery into the NAc was essentially performed as described [19]. The following three viruses were utilized at concentrations from  $2 \times 10^{10}$  (OE, KD) to  $6 \times 10^{11}$  (GFP) particles \* ml<sup>-1</sup>: pAAV.1-CAG-GFP (#37825, Addgene), OE-Npbwr1-GFP: pAAV-CAG-GFP-P2A-Npbwr1-WPRE1, KD-Npbwr1-GFP: pAAV-U6-shRNA-Npbwr1#1-CAG-GFP-P2A-WPR3. Npbwr1-regulating AAVs were custom-made by Charité viral vector core, Berlin, Germany. All AAVs were serotype 1.

### Behavioral tests and CVS

A combination of the acute behavioral tests forced swim test, tail suspension test, sucrose preference, and splash test was performed as described with a combination of at least two tests per experiment [10, 20]. After CVS, no tail suspension test was conducted, as the tail suspension is part of the stress-induction protocol. For CVS groups, caffeine was injected on the last day of CVS (day 21), just before stress induction. The CVS protocol was performed as described [10]. In brief, mice received 21 days of stress with one of three stressors presented in a semi-random order, where the same stressor does not occur on two consecutive days. Stressors consist of 1 h of either, tube restraint, tail suspension, or 100 mild electric random foot shocks. If only female experimenters were present, a used male t-shirt was wrapped in clean protective clothing from the animal unit and placed in the experimental room to avoid variability due to the sex-specific scents of the scientists [21]. Open-field and rotarod tests were performed as previously described [22]. All experiments were conducted in the active phase (dark phase, under red light) of the light cycle.

### Dendritic spine analysis

The analysis was based on detecting the AAVs' GFP-fluorophores. Photos of 40 μm PFA-fixed brain sections were taken with a Zeiss LSM 880 confocal microscope using the AiryScan method. Maximum intensity projections were obtained using Zen Black and Zen Blue software and analyzed in NeuronStudio (CNIC, Mount Sinai School of Medicine). The total density of spines, proportions of neck-containing and stubby spines as well as the cumulative neck length were determined in Graph Prism.

### Next-generation RNA-sequencing

No rRNA depletion was performed but poly-A-enriched mRNAs were sequenced. A total of 500 ng RNA input material per sample was processed using an NEBNext Ultra II Directional RNA Library Preparation Kit (#E7760) in combination with NEBNext Poly(A) mRNA Magnetic Isolation Module (#E7490) and NEBNext Multiplex Oligos for Illumina (Unique Dual Index UMI Adaptors RNA) (#E7416) following the manufacturer's instructions (all New England Biolabs). A final amplification of the library was performed. An in-house RNA-sequencing analysis pipeline was applied as described (<https://github.com/Hoffmann-Lab/rippchen>). We utilized Trimmomatic [23] v0.39 (5nt sliding window, mean quality cutoff 20) for read quality trimming. According to FastQC v0.11.9 reports, the Illumina universal adapter was clipped off the 3' reads end using Cutadapt [24] v2.10. Sequencing errors were detected and corrected using Rcorrector [25] v1.0.4. Ribosomal RNA-derived sequences were artificially depleted by utilizing SortMeRNA [26] v2.1. Subsequently, the data was aligned to the mouse reference genome GRCm38 (mm10) with segemehl [27, 28] v0.3.4 in splice-aware mode and accuracy cutoff raised to 95%. For single-end data with unique molecular identifiers, next to the extraction of unambiguously aligned reads, mappings were further deduplicated for over-amplified PCR fragments utilizing UMI-tools [29] v1.1.1. Afterwards, alignments were quantified on Ensembl v102 reference annotation via featureCounts [30] v2.0.1 (exon-based meta-feature, minimum overlap 10nt). Therefore, strandedness of the library was prior inferred using RSeQC [31] v4.0.0. DESeq2 [32] v1.34.0 was then applied to test for differentially expressed genes. Only significant results (adjusted *P*-value < 0.05, log<sub>2</sub>FC 0.5 < > -0.5) were considered in downstream analyses and interpretations. Data tables are provided in the supplementary tables and via the Gene Expression Omnibus (GEO) database together with raw sequencing data under accession number GSE271600.

### Postmortem samples

Experiments were conducted in agreement with the Ethics Committee of Jena University Hospital, Germany (Reg.-Nr. 2020-1862-Material). Groups were balanced for age and postmortem interval. NAc samples with age <22–80< years and postmortem interval >130 h were excluded. Informed consent was obtained from all subjects. The RNA IQ score was determined using the Qubit RNA IQ Assay-kit (#Q33221, Thermo Fisher Scientific).

### Statistics

Statistical analysis was performed in GraphPrism. Two-tailed Student's *t*-test was used for the comparison of two groups. If variances were unequal, Welch correction was used. In case a Gaussian distribution could not be assumed (e.g. due to a floor effect while reducing already low gene expression to almost zero), the Mann-Whitney-test was used. For the combined data set of both sexes, samples of each sex were normalized to the respective controls to set all controls to an average of 1. One-way ANOVA and Tukey *post hoc* test were used when one factor was varied. Two-way ANOVA and Bonferroni *post hoc* test were used when two factors were varied. The cumulative head diameter of dendritic spines was analyzed using the Gehan-Breslow-Wilcoxon test [16]. Outliers were removed when the data points were more than two standard deviations away from the average. An exception was the postmortem analysis, where samples were excluded before analysis based on extreme age or postmortem interval values to avoid age/postmortem biases between data sets. During behavioral tests and dendritic spine analysis, the experimenters were blind to groups.

Experiments were typically performed only once to minimize animal numbers. However, to increase robustness, a variety of tests and measures was applied (e.g. various behavioral tests, morphology, molecular analysis). Moreover, certain conditions such as CVS were performed in more than one experiment, leading to partial replication. Key experiments, e.g. from RNA-sequencing, were validated in a different cohort using another method (qPCR).

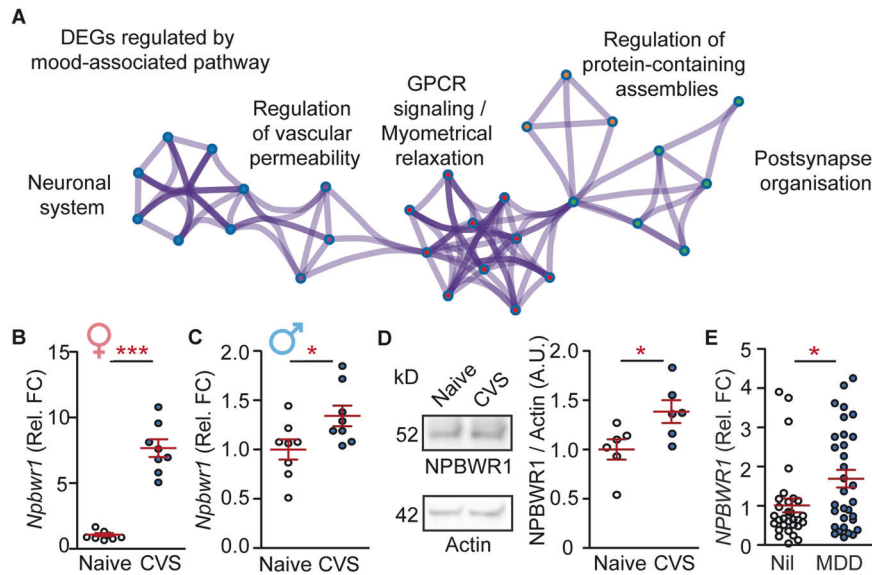


**Fig. 1** *Npbwr1* is associated with chronic stress and depression. **A** Metascape pathway analysis of caffeine-regulated DEGs in the active phase as detected by RNA-sequencing. **B, C** *Npbwr1* levels are increased after chronic variable stress (CVS). **B** Females:  $n = 8$ ; Unpaired t-test with Welch's correction:  $t_7 = 9.71$ ,  $df = 7$ ;  $***P < 0.0001$ . **C** Males:  $n = 8$ ;  $t_{14} = 2.34$ ,  $*P < 0.05$ . **D** NPBWR1 protein levels are elevated after CVS:  $n = 6$ ;  $t_{10} = 2.47$ ,  $*P < 0.05$ . **E** NPBWR1 is increased in depressed patients (MDD) vs. controls (Nil):  $n = 30,32$ ;  $t_{60} = 2.36$ ,  $*P < 0.05$ . **B–E** Independent data points are plotted and means  $\pm$  s.e.m. are shown. DEGs differentially expressed genes. Non-significant comparisons are not listed unless specified. Sketches were generated with biorender.com.

## RESULTS

### *Npbwr1* is increased by chronic stress, elevated in depressed patients and quickly reduced by caffeine

We recently identified a diurnal signaling cascade in the NAC that mediates the effects of caffeine via T75-DARPP-32:CLOCK/BMAL1 interaction on mood [12]. To identify genetic downstream targets of caffeine that may be relevant to mood and associated disorders, we performed next-generation RNA sequencing on NAC tissue of male wildtype (WT) and T75A-DARPP-32 mice (Supplementary Figs. S1 and S2). Consistent with previous data, we observed that most caffeine-induced transcriptional changes occurred in WT at the end of the active (dark) phase (Supplementary Fig. S1, Supplementary Table S1). Altered transcripts belonged to a variety of cellular signaling pathways as predicted by Metascape [33], including neuronal system, postsynapse organization, and negative regulation of vascular permeability (Fig. 1A). Among those, *Npbwr1* was altered by caffeine in WT mice, but not in T75A-DARPP-32 mutant mice at the end of the dark phase, and this was confirmed in an independent cohort (Supplementary Fig. S1).

Given the impact of caffeine on mood, we tested its effect in the CVS model (Supplementary Fig. S3). Briefly, CVS comprises 21 days of daily stress consisting of either 1 h tube restraint, 1 h tail suspension, or 100 random mild electric shocks during 1 h. Our observations indicated that caffeine improved CVS-induced behaviors and reversed morphological changes in the NAC (Supplementary Fig. S3). Therefore, we assessed, whether chronic stress may be associated with altered *Npbwr1* levels. To that end, we employed the CVS model, which allows for a sex-specific intervention and mimics transcriptomic signatures of depression [9, 10]. The expression of *Npbwr1* was increased after CVS in both sexes, however the effect was more pronounced in females (Fig. 1B, C). Additionally, NPBWR1 protein levels were increased after CVS (Fig. 1D, Supplementary Fig. S4). Next, we examined whether NPBWR1 levels were affected postmortem in depressed patients. As expected, obtainable postmortem samples varied in PMI and age (Supplementary Fig. S5). We did not observe correlations between NPBWR1 and PMI ( $R^2 = 0.02$ ,  $P = 0.44$ ), or NPBWR1 and age ( $R^2 = 0.06$ ,  $P = 0.37$ ). The transcription of NPBWR1 was increased in the NAC of postmortem tissue from depressed

patients of both sexes (Fig. 1E, Supplementary Fig. S5). These data suggest that *Npbwr1* is associated with mood and depression and can be altered using the CVS model. *Npbwr1* expression was particularly increased in depressed patients who died from natural causes rather than suicide (Supplementary Fig. S5). The blunted effect in suicide victims may arise due to the anxiety, acute stress, or relief of conducting the act, the acute drug intake often accompanying suicide or other mental conditions associated with it.

### Viral overexpression of *Npbwr1* affects dendritic spines, *Bdnf*, and stress-induced behaviors

To investigate whether *Npbwr1* is causally linked to morphological and behavioral consequences of stress, we obtained genetically modified AAVs to overexpress (OE) or knockdown (KD) *Npbwr1* in the NAC (Figs. 2 and 3; Supplementary Fig. S6). We continued experiments only in female mice, giving the stronger effect size and in turn, the need for fewer animals. OE-*Npbwr1* in the NAC did not affect weight, locomotor skills in the rotarod tests, or anxiety in the open-field paradigm (Supplementary Fig. S7).

OE of *Npbwr1* mimicked chronic stress effects on behavior and dendritic spine density. Specifically, OE-*Npbwr1* (Fig. 2A–D) reduced escape behavior in the forced swim test (Fig. 2E), decreased the time spent grooming in the splash test (Fig. 2F), and the amount of sucrose solution vs. water consumed (Fig. 2G).

Dendritic spines are functionally relevant, morphological correlates of chronic stress and depression [34]. In the NAC, chronic stress is associated with an increase in dendritic spine density on medium-spiny neurons, predominantly on smaller spine types [34]. Consistent with the literature, we observed an increase in spine density after CVS and a reversal by caffeine when analyzing AAV-mediated GFP signals in NAC medium-spiny neurons (Supplementary Figs. S3 and S8A).

Accordingly, OE-*Npbwr1* increased the density of neck-containing spines (Fig. 2H–J). The cumulative head diameter was reduced by OE-*Npbwr1* (Fig. 2K, Supplementary Fig. S8B), indicating an increase in neck-containing spines with small head diameters ("thin" spines).

Next, we were interested in *Npbwr1*-downstream signaling, which is virtually unknown. To that end, we performed RNA-

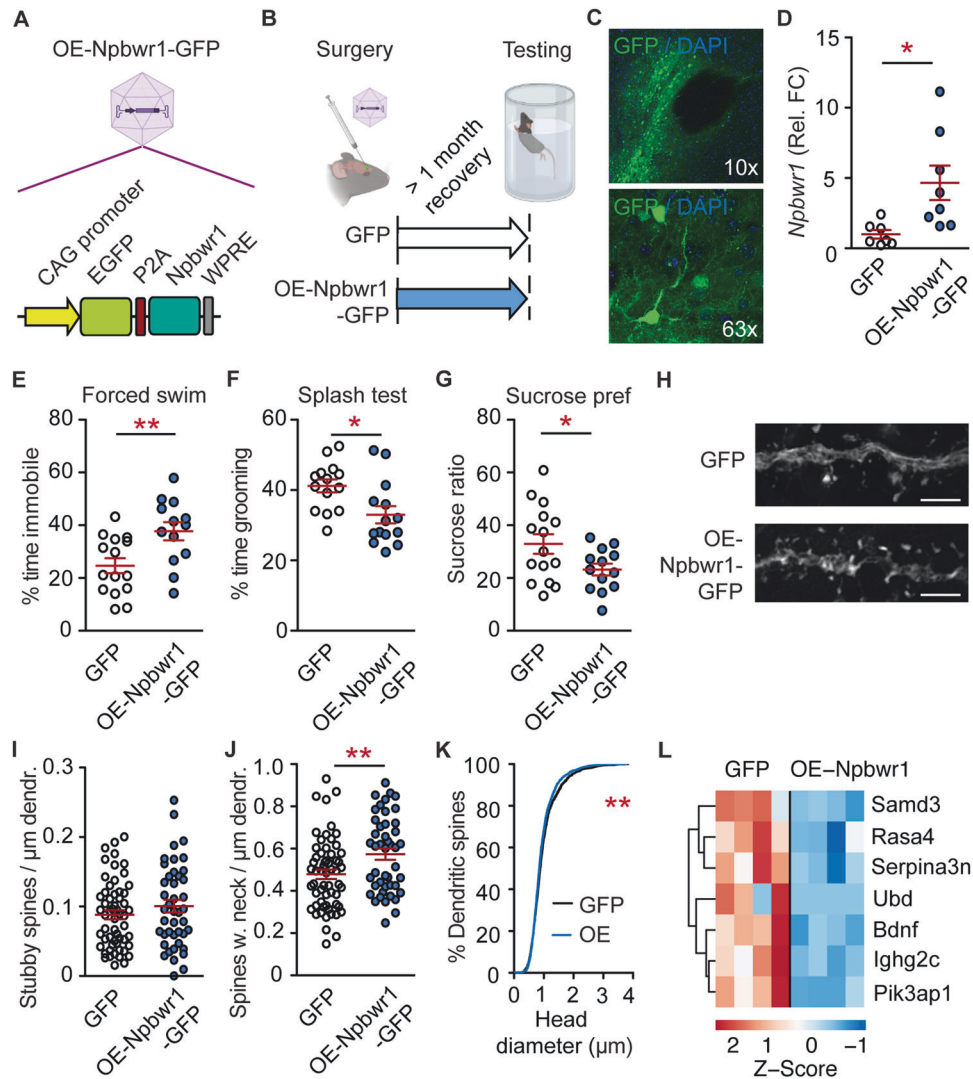


**Fig. 2** Overexpression of *Npbwr1* mimics stress effects on behavior and dendritic spines. **A** Schematic of the OE-*Npbwr1*-GFP AAV. **B** Experimental design. **C** Overview image of viral injection into the NAC. Note the unlabelled anterior commissure as a landmark for the NAC in the upper image. **D** qPCR.  $n = 7,8$ ; Unpaired t-test with Welch's correction:  $t_7 = 2.89$ ,  $*P < 0.05$ . **E–I** Depressive-like behaviors are increased by overexpression (OE) of *Npbwr1*. **E** Increased immobility time in the forced swim test.  $n = 15,13$ ;  $t_{26} = 3.00$ ,  $***P < 0.01$ . **F** Reduced grooming in the splash test.  $n = 14$ ;  $t_{26} = 2.68$ ,  $*P < 0.05$ . **G** Decreased sucrose preference.  $n = 15,13$ ;  $t_{26} = 2.15$ ,  $P > 0.05$ . **H–K** Dendritic spines in the NAC upon OE-*Npbwr1* resemble findings of CVS. **H** Representative dendrites. Scale bar 10  $\mu\text{m}$ . **I** No change in stubby spine density.  $n = 57,43$  from 6,5 mice;  $t_{98} = 1.13$ ,  $P = 0.26$ . **J** More neck-containing spines.  $n = 59,45$  from 6,5 mice;  $t_{102} = 2.76$ ,  $***P < 0.01$ . **K** Increased cumulative head diameter.  $\chi^2 = 7.83$ ,  $df = 1$ ,  $***P < 0.01$ . **L** Heatmap of RNA-sequencing on NAC-tissue from mice infected with OE-*Npbwr1*-GFP virus or GFP-control identified *Bdnf* as *Npbwr1*-regulated gene. **D–G, I, J** Independent data points are plotted and means  $\pm$  s.e.m. are shown. Sketches were made with biorender.com.

sequencing on NAC tissue that was injected with OE-*Npbwr1* AAV or a GFP-expressing control. Surprisingly, only 7 genes were altered (Fig. 2L, Supplementary Table S2). Among them, Brain-derived neurotrophic factor (*Bdnf*) was selected for further investigation because it is highly associated with depression and the antidepressant response [15].

### The knockdown of *Npwr1* prevents the effects of chronic stress

To probe a bidirectional causality of *Npbwr1* on stress effects, we also knocked down *Npbwr1* (Fig. 3A–D). Given the low baseline levels of *Npbwr1* in unstressed mice, we hypothesized that KD of *Npbwr1* may show more pronounced effects in mice that have undergone CVS.

KD-*Npbwr1* did not affect weight, performance on the rotarod, or movement patterns in the open-field paradigm (Supplementary Fig. S7). In contrast, KD-*Npbwr1* prevented the consequences of

CVS in the forced swim test (Fig. 3E) and on dendritic spine morphology, specifically on neck-containing spines (Fig. 3F, G; Supplementary Fig. S8C). Consistently with Fig. 2 and Supplementary Fig. S3, no change in stubby spine density was detected (data not shown). Moreover, in agreement with Fig. 2, CVS reduced the cumulative head diameter and this was prevented by KD-*Npbwr1* (Fig. 3H–K).

In summary, these data further demonstrate a causal link between long-term changes in *Npbwr1* and depression-associated symptoms. However, the AAV-based experimental approach cannot reflect a fast modulation of *Npbwr1* signaling.

### Microinjection of *Npbwr1* ligands rapidly alters depressive-like behaviors

To address the fast-acting aspect of the *Npbwr1* pathway, we microinjected ligands into the NAC that either activate

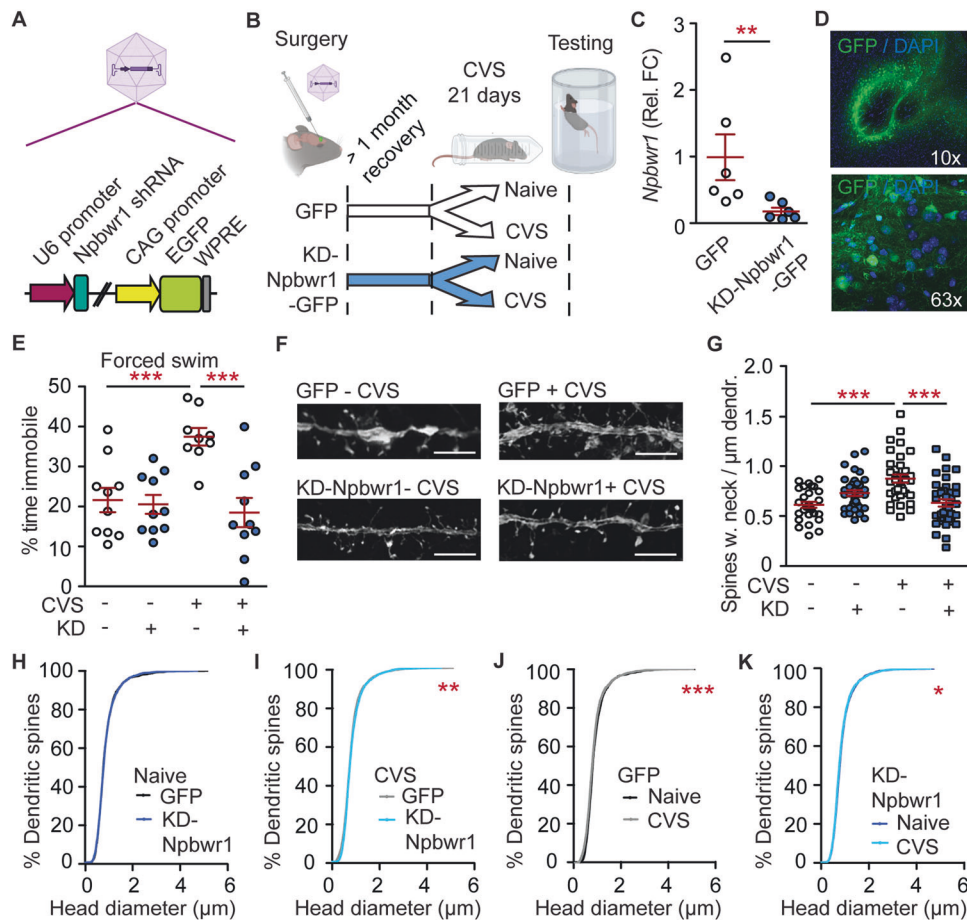


**Fig. 3** Knockdown of *Npbwr1* blocks the effects of CVS on behavior and dendritic spines. **A** Schematic of the KD-*Npbwr1*-GFP AAV. **B** Experimental plan. **C** qPCR (naive mice): qPCR.  $n = 6$ ; Mann-Whitney test:  $**P < 0.01$ . **D** Overview image of viral injection into the NAC. **E** KD reverses the stress effect in the forced swim test.  $n = 10, 10, 9, 10$ ; stress effect:  $F(1, 35) = 6.24$ ,  $P < 0.05$ ; AAV effect:  $F(1, 35) = 13.21$ ,  $P < 0.001$ ; interaction:  $F(1, 35) = 10.50$ ,  $P < 0.01$ ; *post hoc* test: AAV effect within CVS:  $***P < 0.001$ ; stress effect within GFP:  $***P < 0.001$ . **F** Representative dendrites. Scale bar 10  $\mu\text{m}$ . **G** Neck-containing spines.  $n = 28, 36, 34, 37$  dendrites from 3, 4, 4, 4 mice; stress effect:  $F(1, 131) = 5.35$ ,  $P < 0.05$ ; interaction:  $F(1, 131) = 25.85$ ,  $P < 0.0001$ ; *post hoc* test: AAV effect within CVS:  $***P > 0.001$ , within naive:  $*P < 0.05$ ; stress effect within GFP:  $***P < 0.001$ . **H-K** The cumulative head diameter, is reduced by CVS and rescued by KD-*Npbwr1*; **H** AAV effect within naive:  $\chi^2 < 0.01$ ,  $df = 1$ ,  $P = 0.96$ . **I** AAV effect within CVS:  $\chi^2 = 7.71$ ,  $df = 1$ ,  $**P < 0.01$ . **J** Stress effect within GFP:  $\chi^2 = 20.05$ ,  $df = 1$ ,  $***P < 0.0001$ . **K** Stress effect within KD:  $\chi^2 = 4.58$ ,  $df = 1$ ,  $*P < 0.05$ . **C**, **E**, **G** Independent data points are plotted and means  $\pm$  s.e.m. are shown. Non-significant comparisons are not listed unless specified. Sketches were made with biorender.com.

(neuropeptide B, NPB) or inhibit (CYM50769) *Npbwr1*. While NPB is a natural neurotransmitter, CYM50769 is a synthetic ligand, which has not yet been tested *in vivo*. Hence, dosing, selectivity, and toxicity were assessed first. Doses of CYM50769 up to 10  $\mu\text{M}$  were injected into the NAc and mice were scored for 7 days. No effects on body weight, hydration status, cramps or stereotypies, respiration, coordination, fur, auto-mutilation, locomotor activity, or posture were observed (data not shown). The lowest ligand concentrations with the clearest effects on *Bdnf* were further tested (1  $\mu\text{M}$  CYM50769, 1 nM NPB). CYM50769 and NPB altered *Bdnf* levels in the NAc, as expected in opposite directions (Fig. 4A–C). Importantly, *Bdnf* was still altered 7 days after a single injection of CYM50769 (Fig. 4D). Neither NPB nor CYM50769 affected the apoptosis markers *Bcl2* and *Casp3* thus ruling out neurotoxicity. Moreover, they did not alter levels of the circadian gene *Per2*, suggesting a selective action of these ligands (Supplementary Fig. S9).

Next, we tested the rapid effects of *Npbwr1* activity on depressive-like behaviors. To this end, mice underwent CVS and received 1 nM NPB and 1  $\mu\text{M}$  CYM50769 after the last session of stress induction. Behavioral tests were conducted app. 24 h later. We observed that NPB aggravated depressive-like behaviors in

naive mice in the forced swim, splash, and sucrose preference tests, while not enhancing the behavioral effects of CVS further (Fig. 4E–G). In contrast, CYM50769 had no effects in naive mice. However, CYM50769 rapidly rescued CVS-induced behavioral symptoms in all tests (Fig. 4E–G). To make our data more applicable to both sexes, the impact of CYM50769 on stress-induced behaviors in males was assessed in the two tests, which showed the clearest results in females, the forced swim test, and the sucrose preference test. In males, too, CYM50769 reversed stress-induced changes in immobility time in the forced swim test and prevented stress effects in the sucrose preference test (Supplementary Fig. S10). Hence, CYM50769 rapidly improves stress-induced behavioral changes in both sexes.

These data are consistent with the effects of viral-mediated overexpression and knockdown of *Npbwr1* levels (Figs. 2 and 3; Supplementary Fig. S11). They also indicate fast-acting effects of CYM50769 ligands on depressive-like behaviors, at least in mice. Given the rapid reversal of stress-induced symptoms, the persistence of *Bdnf* changes for 7 days, and the excellent tolerability in our studies, CYM50769 deserves further investigation for its role in ameliorating symptoms related to chronic stress and depression.

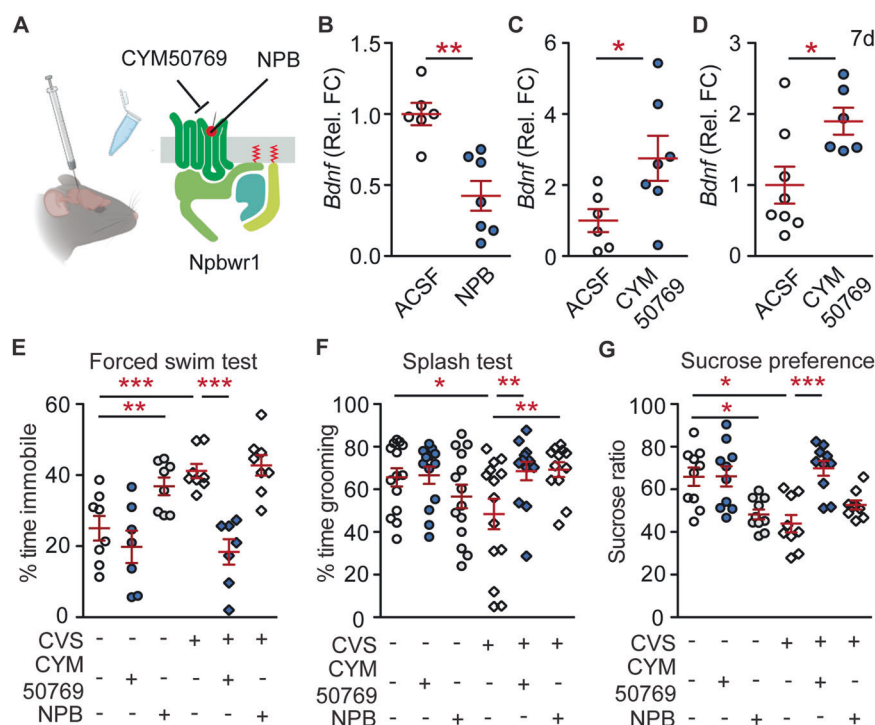


**Fig. 4** *Npbwr1*-ligands alter *Bdnf* signaling and improve depressive-like behaviors. **A** Overview of ligand binding of the agonist neuropeptide B (NPB) and the antagonist CYM50769 to *Npbwr1*. **B** 1 nmolar NPB or **C**, **D** 1  $\mu$ molar CYM50769 or was microinjected and tissue was collected 24 h (**B**, **C**) or 7 days later (**D**) and analyzed by qPCR. **B** NPB decreases *Bdnf* 24 h after injection.  $n = 6,7$ ,  $t_{11} = 4.28$ ,  $P < 0.01^{**}$ . **C** CYM50769 increases *Bdnf* 24 h after injection.  $n = 6,7$ ,  $t_{11} = 2.34$ ,  $P < 0.05^*$ . **D** CYM50769 effect on *Bdnf* persists at the 7-day time point.  $n = 8,6$ ,  $t_{12} = 2.61$ ,  $P < 0.05^*$ . **E–G** Mice underwent CVS (vs. naïve controls) and were microinjected with NPB or CYM50769 at the end of the active phase after the last stress induction. Tests for depressive-like behavior were conducted app. 24 h later in the dark phase. **E** Forced swim test. NPB increases the immobility time in naïve mice, while CYM50769 blocks CVS effects.  $n = 8,7,8,8,7,8$ ; CVS effect:  $F(1,46) = 6.47$ ,  $P < 0.05$ ; ligand effect:  $F(2,46) = 23.80$ ,  $P < 0.001$ ; interaction:  $F(2,46) = 5.05$ ,  $P < 0.05$ ; *post hoc* test: stress effect within ACSF:  $^{***}P < 0.001$ ; NPB effect within naïve:  $^{**}P < 0.01$ ; CYM50769 effect within CVS:  $^{***}P < 0.001$ . **F** Splash test. NPB may reduce grooming in naïve mice, while CYM50769 blocks CVS effects.  $n = 14,13,14,14,13,12$ ; interaction:  $F(2,74) = 4.83$ ,  $P < 0.05$ . *Post hoc* test: CVS effect within ACSF:  $^*P < 0.05$ ; CYM effect within CVS:  $^{**}P < 0.01$ ; NPB effect within CVS:  $^{***}P < 0.01$ . **G** Sucrose preference. NPB and CVS reduce the ratio of sucrose solution consumed, while CYM50769 rescues CVS effects.  $n = 10,10,10,9,10,9$ ; effect of ligands:  $F(2,50) = 12.86$ ,  $P < 0.0001$ ; interaction:  $F(2,50) = 4.65$ ,  $P < 0.05$ ; *post hoc* test: CVS effect within ACSF:  $^*P < 0.05$ ; NPB effect within naïve:  $^*P < 0.05$ ; CYM50769 effect within CVS:  $^{***}P < 0.001$ . **B–G** Independent data points are plotted and means  $\pm$  s.e.m. are shown. Non-significant comparisons are not listed. Sketches were made with biorender.com.

## DISCUSSION

This study describes a previously unknown pathway, which mediates rapid effects on depressive-like behaviors and stress response via *Npbwr1*. Viral-mediated gene transfer stably altered levels of *Npbwr1*. While overexpression of *Npbwr1* mimicked depressive-like symptoms, its knockdown prevented chronic stress effects without affecting mood in naïve mice. This dichotomous effect may be explained by relatively low baseline levels of *Npbwr1* in the NAc as observed by Cq-values of *Npbwr1* by qPCR of more than 25 in naïve mice. Hence, effects on *Npbwr1* regulation may become apparent when *Npbwr1* levels are upregulated or the activity of *Npbwr1* is increased, e.g. after CVS. Consistently, the regulation of *Npbwr1* activity via microinjection of ligands altered depression-related symptoms depending on a previous CVS induction. Stimulation of *Npbwr1* via NPB induced depressive-like behaviors in naïve mice, while an inhibition with CYM50769 blocked those symptoms within the CVS-cohort.

It is currently unclear how *Npbwr1* signaling mediates downstream effects on gene expression and dendritic spine morphology. Second messenger cascades may affect gene expression, however, only a small number of genes were altered in our RNA sequencing data set from OE-*Npbwr1* and they did not involve synaptic genes. Hence it is likely that other mechanisms such as posttranslational modifications on synaptic proteins and protein-protein interactions near the synaptic cytoskeleton are affected. Dendritic spine morphology is not only regulated by signaling

cascades of the postsynaptic cell but also by synaptic input from the presynaptic cell. The NAc receives inputs from several brain regions including the ventral tegmental area and the prefrontal cortex [35]. In our viral experiments, only the NAc was manipulated, while CVS affects a variety of brain regions [10]. Viral experiments have a long-term trajectory, whereas caffeine has a rapid mode of action. Moreover, a variety of neurotransmitters besides *Npbwr1* ligands are likely to affect dendritic spine morphology. Therefore, while our data are largely internally consistent, they need to be put in a bigger context in the future. Further experiments involving chemogenetic stimulation of specific circuits, as well as stimulation with certain other receptor agonists and antagonists, are planned.

Stress- and caffeine-induced changes in *Npbwr1* levels in other brain regions such as the amygdala or the VTA have not been investigated. Using localized viral and microinjection strategies, we focused on *Npbwr1* function in the NAc. For instance, we do not exclude the possibility that *Npbwr1* may regulate anxiety when manipulated in other brain regions such as the amygdala, or affect weight when manipulated in relevant brain regions such as the hypothalamus. *Npbwr1* function in other brain regions should be studied in more depth in the future, in particular, to predict the side effects of CYM50769 on other behaviors. Moreover, we have not explored, which brain regions produce the natural agonists that stimulate *Npbwr1* in the NAc. Our study on the receptor for neuropeptides B and W sheds new light on this little-explored

neurotransmitter system. This encourages further investigation of neuropeptide systems in the brain as they may mediate disease states via understudied pathways.

Depression is associated with different molecular signatures in males and females and this is reflected by the CVS-mouse model [10]. Accordingly, we observed a 4x stronger effect of CVS on *Npbwr1* levels. Nevertheless, male mice, too, showed increased stress-induced *Npbwr1* levels and they also benefited from CYM50769 administration after CVS. Hence, our data are relevant for both sexes.

Several SNPs are described within the NPBWR1 gene, which are mostly of uncertain significance or have no known link to depression. rs35551581 has been correlated with antidepressant response in one study but was not found to have a clear phenotypical relevance [36]. Other SNPs are associated with smoking and traumatic early childhood events (rs2376427), as well as body mass index (rs7822058-A, rs575733898-T, rs10095724-G), which may be of relevance to observed endophenotypes of altered anhedonia. Interestingly, NPBWR1 is located in the 8q11.23 region, neighboring the RB1CC1 gene, and two NPBWR1 duplications are associated with schizophrenia, making this gene potentially interesting in yet another disease context.

Current and future testing involves the applicability of CYM50769 for oral administration, including PET-tracing of a radioactive version across tissues. Based on the molecular structure it is likely that CYM50769 may cross the blood-brain-barrier and that it may be transiently deposited in fatty tissues, leading to a slow release which may partially explain the observed effects after 7 days (personal communication with Prof. Anna Junker, University of Tübingen, Germany). Based on these data, the original or an adapted molecule will be tested for oral application, dosing regime and efficacy, side effects, and antidepressant effects. Despite observed changes in *Bdnf* levels after 7 days, the effect of an acute dose of CYM50769 is likely transient. This is also suggested by *Npbwr1*-induced changes in dendritic spine morphology, which point toward an alteration in the dynamic and transient "thin" spines, which need reinforcement to develop into more stable mushroom spines. Taken together, it is highly likely that CYM50769, as most compounds, will need to be administered at regular intervals, warranting the testing of cumulative side effects as well.

Guerrero et al. demonstrated a high selectivity of CYM50769 [37]. However, at the high dose of 30  $\mu$ M, they observed a 63% inhibition of the serotonin receptor 5-HT<sub>2B</sub> in the Ricerca panel of off-target proteins. In light of these data, cross-talk with the serotonergic system, in particular during co-administration with selective serotonin reuptake inhibitors, needs to be investigated further.

A main focus of continued studies will be CYM50769's effects on anxiety. Anxiety- and mood disorders show a strong comorbidity. Caffeine can be anxiolytic at low doses but anxiogenic at high doses, and therefore it is plausible that downstream proteins such as *Npbwr1* may contribute to this effect. We did not detect significant effects of virally altered *Npbwr1* levels on anxiety in the open-field test. However, given the importance of this aspect, particularly regarding chronic and acute CYM50769 effects, this will be a focus of in-depth future studies.

In mice, CYM50769 is fast-acting, selective, well tolerated, and showed effects up to 7 days after administration of a single dose. Despite more preclinical testing being required to assess oral applicability, long-term safety, efficacy, and side effects, the data presented here provide new insights regarding our standing of stress response and, possibly, antidepressant action.

## DATA AVAILABILITY

All relevant data are presented within this article or can be accessed within the supplementary information. Raw sequencing data can be obtained via the Gene

Expression Omnibus (GEO) database under accession number GSE271600. Further data regarding this publication may be requested from the corresponding author.

## REFERENCES

- Bebbington P. The World Health Report 2001 - Mental Health: New Understanding. New Hope. Soc Psychiatry Psychiatr Epidemiol. 2001;36:473–4.
- Vos T, Abajobir AA, Hassen Abate K, Abbafati C, Abbas KM, Abd-Allah F, et al. Global, regional, and national incidence, prevalence, and years lived with disability for 328 diseases and injuries for 195 countries, 1990–2016: A systematic analysis for the Global Burden of Disease Study 2016. Lancet. 2017;390:1211–59.
- Lim G, Tam WW, Lu Y, Ho CS, Zhang MW, Ho RC. Prevalence of Depression in the Community from 30 Countries between 1994 and 2014. Sci Rep. 2018;8:2861.
- Tomonaga Y, Haettenschwiler M, Hatzinger M, Holsboer-Trachsler E, Rufer M, Hepp U, et al. The economic burden of depression in Switzerland. Pharmacoeconomics. 2013;31:237–50.
- Greenberg PE, Fournier AA, Sisitsky T, Pike CT, Kessler RC. The economic burden of adults with major depressive disorder in the United States (2005 and 2010). J Clin Psychiatry. 2015;76:155–62.
- Kirsch I, Deacon T, Huedo-Medina TB, Scoboria A, Moore TJ, Johnson BT. Initial severity and antidepressant benefits: a meta-analysis of data submitted to the Food and Drug Administration. PLoS Med. 2008;5:e45.
- Cipriani A, Furukawa G, Salanti G, Chaimani A, Atkinson LZ, Ogawa Y, et al. Comparative efficacy and acceptability of 21 antidepressant drugs for the acute treatment of adults with major depressive disorder: a systematic review and network meta-analysis. Lancet. 2018;391:1357–66.
- Munkholm K, Paludan-Müller A, Boesen K. Considering the methodological limitations in the evidence base of antidepressants for depression: a reanalysis of a network meta-analysis. BMJ Open. 2019;9:e024886.
- Scarpa J, Fatma M, Loh Y, Traore SR, Stefan T, Chen TH, et al. Shared Transcriptional Signatures in Major Depressive Disorder and Mouse Chronic Stress Models. Biol Psychiatry. 2020;88:159–68.
- Labonte B, Engmann O, Purushothaman I, Hodes GE, Lorsch ZS, Hamilton PJ, et al. Sex-Specific Transcriptional Signatures in Human Depression. Nat Med. 2017;23:1102–11.
- Aly J, Engmann O. The Way to a Human's Brain Goes Through Their Stomach: Dietary Factors in Major Depressive Disorder. Front Neurosci. 2020;14:582853.
- Trautmann C, Burek D, Huebner C, Girault J-A, Engmann O. A regulatory pathway linking caffeine action, mood and the diurnal clock. Neuropharmacology. 2020;172:108133.
- Dun SL, Brailoiu K, Mizuo K, Yang J, Chang JK, Dun NJ. Neuropeptide B immunoreactivity in the central nervous system of the rat. Brain Res. 2005;1045:157–63.
- Singh G, Maguire JJ, Kuc RE, Fidock M, Davenport AP. Identification and cellular localisation of NPW1 (GPR7) receptors for the novel neuropeptide W-23 by [125I]-NPW radioligand binding and immunocytochemistry. Brain Res. 2004;1017:222–6.
- Cubillos S, Engmann O, Brancato A. BDNF as a Mediator of Antidepressant Response: Recent Advances and Lifestyle Interactions. Int J Mol Sci. 2022;23:14445.
- Engmann O, Giral A, Gervasi N, Marion-Poll L, Gasmil L, Filhol O, et al. DARPP-32 interaction with adducin may mediate rapid environmental effects on striatal neurons. Nat Commun. 2015;6:10099.
- Lindskog M, Svenningsson P, Pozzi L, Kim Y, Fienberg AA, Bibb JA, et al. Involvement of DARPP-32 phosphorylation in the stimulant action of caffeine. Nature. 2002;418:774–8.
- Trautmann C, Bock A, Urbach A, Hübner A, Engmann O. Acute vitamin B12 supplementation evokes antidepressant response and alters Ntrk-2. Neuropharmacology. 2020;171:108112.
- Wook Koo J, Labonte B, Engmann O, Calipari E, Juarez B, Lorsch Z, et al. Essential Role of Mesolimbic Brain-Derived Neurotrophic Factor in Chronic Social Stress-Induced Depressive Behaviors. Biol Psychiatry. 2015;80:469–78.
- Scott MM, Marcus J, Pettersen A, Birnbaum SG, Mochizuki T, Scammell TE, et al. Hcrtr1 and 2 signaling differentially regulates depression-like behaviors. Behav Brain Res. 2011;222:289–94.
- Sorge RE, Martin L, Isbester KA, Sotocinal SG, Rosen S, Tuttle AH, et al. Olfactory exposure to males, including men, causes stress and related analgesia in rodents. Nat Methods. 2014;11:629–32.
- Engmann O, Hortobagyi T, Pidsley R, Troakes C, Bernstein HG, Kreuz MR, et al. Schizophrenia is associated with dysregulation of a Cdk5 activator that regulates synaptic protein expression and cognition. Brain. 2011;134:2408–21.
- Bolger A, Lohse M, Usadel B. Trimmomatic: a flexible trimmer for Illumina sequence data. Bioinformatics. 2014;30:2114–20.
- Martin M. Cutadapt Removes Adapter Sequences From High-Throughput Sequencing Reads. EMBnetjournal. 2011;17.
- Song L, Florea L. Rcorrector: efficient and accurate error correction for Illumina RNA-seq reads. Gigascience. 2015;4:48.

26. Kopylova E, Noé L, Touzet H. SortMeRNA: fast and accurate filtering of ribosomal RNAs in metatranscriptomic data. *Bioinformatics*. 2012;28:3211–7.
27. Hoffmann S, Otto C, Doose G, Tanzer A, Langenberger D, Christ S, et al. A multi-split mapping algorithm for circular RNA, splicing, trans-splicing and fusion detection. *Genome Biol*. 2014;15:R34.
28. Hoffmann S, Otto C, Kurtz S, Sharma CM, Khativich P, Vogel J, et al. Fast mapping of short sequences with mismatches, insertions and deletions using index structures. *Plos Comput Biol*. 2009;5:e1000502.
29. Smith T, Heger A, Sudbery I. UMI-tools: modeling sequencing errors in Unique Molecular Identifiers to improve quantification accuracy. *Genome Res*. 2017;27:491–9.
30. Liao Y, Smyth G, Shi W. featureCounts: an efficient general purpose program for assigning sequence reads to genomic features. *Bioinformatics*. 2014;30:923–30.
31. Wand L, Wang S, Li W. RSeQC: quality control of RNA-seq experiments. *Bioinformatics*. 2012;28:2184–5.
32. Love M, Huber W, Anders S. Moderated estimation of fold change and dispersion for RNA-seq data with DESeq2. *Genome Biol*. 2014;15:550.
33. Zhou Y, Zhou B, Pache L, Chang M, Khodabakhshi AH, et al. Metascape provides a biologist-oriented resource for the analysis of systems-level datasets. *Nat Commun*. 2019;10:1523.
34. Duman C, Duman R. Spine synapse remodeling in the pathophysiology and treatment of depression. *Neurosci Lett*. 2015;601:20–29.
35. Nestler E, Russo S. Neurobiological basis of stress resilience. *Neuron*. 2024;112:1911–29.
36. Fabbri C, Tansey KE, Perlis RH, Hauser J, Heningsberg N, Maier W, et al. New insights into the pharmacogenomics of antidepressant response from the GEN-DEP and STAR\*D studies: rare variant analysis and high-density imputation. *Pharmacogenomics*. 2018;18:413–21.
37. Guerrero M, Urbano M, Schaeffer MT, Brown S, Rosen H, Roberts E. SAR analysis of novel non-peptidic NPBWR1 (GPR7) antagonists. *Bioorganic Med Chem Lett*. 2013;23:614–9.

## ACKNOWLEDGEMENTS

This study was supported by an Advanced Medical Scientist Award from the Interdisciplinary Center for Clinical Research (IZKF) at the Jena University Hospital, Germany (#973685). Furthermore, this project was made possible by funding from the Carl-Zeiss-Foundation (IMPULS #P2019-01-0006). We thank Dr. Thorsten Trimbuch and the Team of the Viral Core Facility of the Charité - Universitätsmedizin Berlin ([vcf.charite.de](http://vcf.charite.de)) for providing inputs and reagents for the AAV experiments and Sabine Grunauer-Vasconez (Friedrich-Schiller-University, Jena, Germany) for help with dendritic spine analysis. The Core Facility “Next Generation Sequencing” headed by Dr. Marco Groth of the FLI is gratefully acknowledged for their technological support. The FLI is a member of the Leibniz Association and is financially supported by the Federal Government of Germany and the State of Thuringia. Before publication, this paper was made publicly available on *BioRxiv.org*.

## AUTHOR CONTRIBUTIONS

GS, JSA, LL and OE performed mouse experiments and analysis. GS, LL and OE planned experiments and handled paperwork involving animal experiments. GS double-checked data and statistics. JSA, OE and AM analyzed dendritic spines. KR and SH analyzed the RNA-sequencing data. AB helped with experimental design. GT provided human postmortem samples. CAH provided infrastructure, and conceptual advice and edited the manuscript. OE designed and planned the study, obtained funding and wrote the article.

## FUNDING

Open Access funding enabled and organized by Projekt DEAL.

## COMPETING INTERESTS

Based on the data presented in this publication, the corresponding author filled the following patent application EP23192592 “Neuropeptide B and W-receptor as a target for treating mood disorders and/or chronic stress” via Friedrich-Schiller-University, Jena, Germany.

## ADDITIONAL INFORMATION

**Supplementary information** The online version contains supplementary material available at <https://doi.org/10.1038/s41380-024-02790-4>.

**Correspondence** and requests for materials should be addressed to Olivia Engmann.

**Reprints and permission information** is available at <http://www.nature.com/reprints>

**Publisher’s note** Springer Nature remains neutral with regard to jurisdictional claims in published maps and institutional affiliations.



**Open Access** This article is licensed under a Creative Commons Attribution 4.0 International License, which permits use, sharing, adaptation, distribution and reproduction in any medium or format, as long as you give appropriate credit to the original author(s) and the source, provide a link to the Creative Commons licence, and indicate if changes were made. The images or other third party material in this article are included in the article’s Creative Commons licence, unless indicated otherwise in a credit line to the material. If material is not included in the article’s Creative Commons licence and your intended use is not permitted by statutory regulation or exceeds the permitted use, you will need to obtain permission directly from the copyright holder. To view a copy of this licence, visit <http://creativecommons.org/licenses/by/4.0/>.

© The Author(s) 2024